Calibration of the Purple Crow Lidar vibrational Raman water-vapour mixing ratio and temperature measurements[1]

P.S. Argall, R.J. Sica, C.R. Bryant, M. Algara-Siller, and H. Schijns

Abstract: Purple Crow Lidar (PCL) measurements of the vibrational Raman-shifted backscatter from water vapour and nitrogen molecules allows height profiles of the water-vapour mixing ratio to be measured from 500 m up into the lower stratosphere. In addition, the Raman nitrogen measurements allow the determination of temperature profiles from about 10 to 40 km altitude. However, external calibration of these measurements is necessary to compensate for instrumental effects, uncertainties in our knowledge of the relevant molecular cross sections, and atmospheric transmission. A comparison of the PCL-derived water-vapour concentration and temperature profiles with routine radiosonde measurements from Detroit and Buffalo on 37 and 141 nights, respectively, was undertaken to provide this calibration. The calibration is then applied to the measurements and monthly mean-temperature and water-vapour profiles are determined.

PACS Nos.: 42.68.Wt, 42.79.Qx

Résumé : Les mesures lidar de Purple Crow (PCL) par rétrodiffusion des vibrations à déplacement Raman dans la vapeur d'eau et l'azote moléculaire dans l'atmosphère permettent de déterminer les profils en altitude du rapport de mélange de vapeur d'eau de 500 m jusqu'à la basse stratosphère. De plus, les mesures Raman sur l'azote permettent de déterminer les profils de température entre 10 km et 40 km. Cependant, une calibration externe de ces mesures est nécessaire pour compenser les effets instrumentaux, les incertitudes sur les sections efficaces impliquées et la transmission atmosphérique. Cette calibration a été effectuée en comparant les concentrations de vapeur d'eau de PCL avec celles faites de façon routinière de Détroit et de Buffalo pendant 37 et 141 nuits respectivement. Nous appliquons ensuite cette calibration aux mesures et déterminons les températures mensuelles moyennes et les profils de vapeur d'eau.

[Traduit par la Rédaction]

Received 30 January 2006. Accepted 14 October 2006. Published on the NRC Research Press Web site at http://cjp.nrc.ca/ on 5 April 2007.

P.S. Argall,[2] R.J. Sica, C.R. Bryant, M. Algara-Siller, and H. Schijns. Department of Physics and Astronomy, The University of Western Ontario, London, ON N6A 3K7, Canada.

[1]This paper is published as part of the proceedings of the Atmospheric Studies by Optical Methods (ASOM) conference that was held 29 August to 1 September 2005 at the University of Western Ontario, London, Ont.

[2]Corresponding author (e-mail: pargall@uwo.ca).

 doi: 10.1139/P06-091 © 2007 NRC Canada

Introduction

The University of Western Ontario's Purple Crow Lidar (PCL) is a powerful Rayleigh, resonance-scatter and Raman lidar system. The transmitter for the Rayleigh and Raman channels uses a frequency-doubled YAG laser, which produces 600 mJ pulses at a pulse-repetition-frequency of 20 Hz, i.e., 12 W average power, at a wavelength of 532 nm. The PCL receiver is based on a 2.65 m diameter liquid mercury mirror [1]. Separate detection system channels record the backscatter intensity profiles for the two Raman channels, molecular nitrogen, and water vapour, in addition to the high-altitude Rayleigh scatter and sodium resonance channels.

In addition to elastic backscatter, which occurs when the scattering molecules quantum state is unaffected by the scattering process, there is a smaller probability that the scattering may be inelastic causing a change in the vibrational and (or) rotational level of the scattering molecule. If this occurs, there will be an appropriate difference in the energy of the incident and scattered photons. Molecular vibrational energy levels are separated much more widely than rotational levels so that vibrational Raman scattering leads to greater wavelength shifts of the scattered light than rotational Raman scattering.

Because of the unique energy level structure of each molecular species the Raman shift produced by each species will also be unique. This allows the identification of the Raman backscatter from each type of molecule by its wavelength. The first vibrational Stokes shift for water vapour is 3651.7 cm^{-1} and for nitrogen 2330.7 cm^{-1}. When illuminated with 532 nm light, water-vapour molecules will cause vibrational Raman scattering at 660 nm and nitrogen at 607 nm. The first demonstrations of lidar utilizing Raman scattering were in the late 1960s [2, 3].

The PCL uses dichroic mirrors to separate the backscattered elastic light and the two Raman-shifted wavelengths of interest. The cross section for the Raman scattering from nitrogen is 1150 times smaller than that for elastic scattering, for water vapour it is 510 times smaller.

Figure 1 shows a schematic of the PCL detection system indicating the way in which the received light is distributed to the various detection channels.

Rayleigh lidar can be used to determine temperature profiles from the upper stratosphere (around 30 km altitude) to the lower thermosphere. Temperature profiles are calculated from measurements of the backscattered intensity, which is proportional to density. Using a measured relative density profile an absolute temperature profile can be determined [4–6]. The lower altitude limit for this technique is imposed by the presence of the stratospheric aerosol layer. The aerosols in this layer, which is typically limited to altitudes below 30 km, also scatter the incident laser light and add to the molecular scatter signal so that the measured backscatter intensity profile from within the aerosol layer is not proportional to the atmospheric density. This means that temperature cannot be determined in the altitude ranges in which aerosol scattering occurs. The vibrational Raman scatter from nitrogen molecules is spectrally well-separated from the elastic aerosol scattering and can be measured without direct contamination by aerosol scattering. As nitrogen is well mixed in the atmosphere, the measured Raman nitrogen backscatter intensity profile is proportional to the atmospheric density and allows the calculation of a temperature profile. However, in the lower 30 km of the atmosphere the optical attenuation, due to both molecular and aerosol scattering and absorption, is significant and a correction needs to be applied to obtain a density profile from a measured photon-count profile. It is the attenuation from one lidar range bin to the next that is important for this correction and not the attenuation from the lidar to each range bin. Rayleigh lidar temperature profiles can be determined without the lidar requiring external calibration, however, vibrational Raman temperature lidar is affected by atmospheric optical transmission and in the case of the PCL, by the changing efficiency of the receiver system with range and so does require external height-dependent calibration. As the Rayleigh lidar temperature profiles do not cover the same altitude range as the Raman temperature profiles they cannot be used to calibrate the Raman temperature lidar.

The optical attenuation in the troposphere is quite variable over even short time scales. However, the attenuation in the stratosphere is generally less variable expect for a period of several months to

© 2007 NRC Canada

Fig. 1. Schematic of the PCL optical detection system.

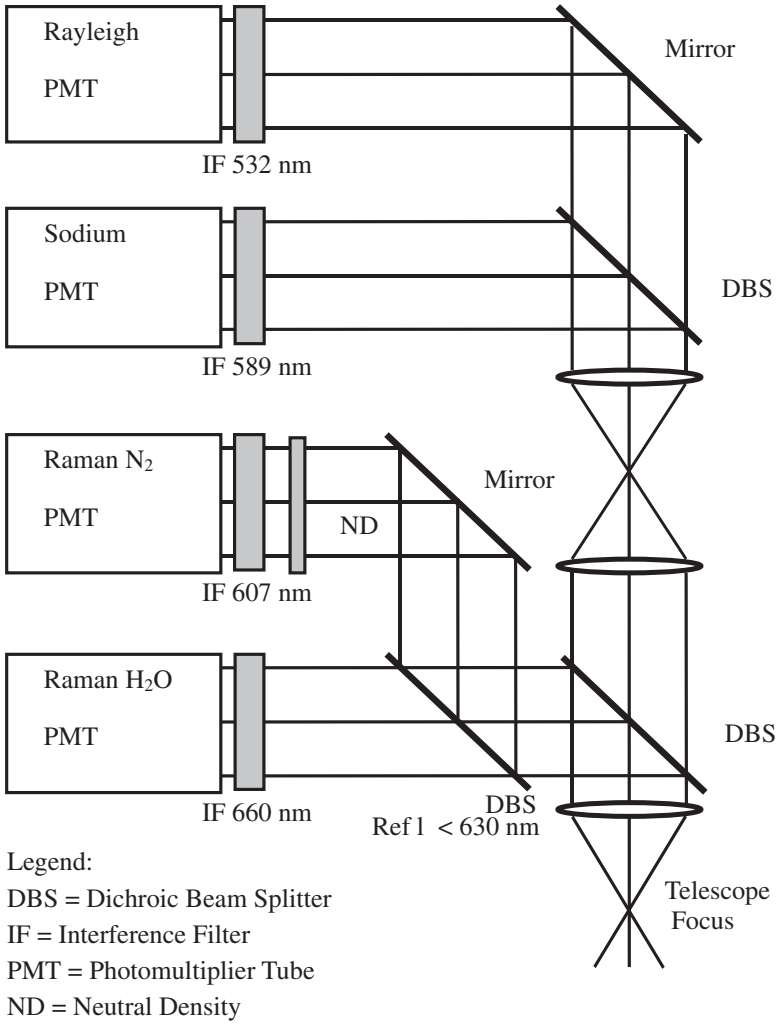

a few years after a major volcanic eruption such as Mount Pinatubo in 1991. During periods when the stratospheric aerosol layer is unperturbed by volcanic activity, a single correction to the Raman-backscatter profile can be used to obtain a relative density profile down to about 10 km altitude [7].

The measurement of tropospheric water-vapour concentration profiles also requires an external calibration but for a different reason. Measuring the intensity profile of the Raman backscatter from water vapour molecules does not provide sufficient information to allow the determination of water vapour concentrations without an absolute calibration of the lidar system and knowledge of the atmospheric transmitance. Determination of the water-vapour concentration is much simpler if along with the Raman scattering from water vapour the Raman nitrogen signal is also measured and the result expressed as a mass- or volume-mixing ratio. Changes in the optical efficiency of the lidar detection system with range, and atmospheric optical attenuation, cause range-dependent variations in the measured backscatter profile. A first-order correction due to these effects can be determined by normalizing the Raman water-vapour profile with a coincident Raman nitrogen profile.

However, the optical attenuation of the atmosphere is different at the wavelengths of the water-vapour and nitrogen Raman backscatter. In addition, the optical efficiency of the lidar detection system

© 2007 NRC Canada

Fig. 2. The average-temperature difference between the US and Delaware radiosondes as a function of altitude. The error bars represent the variability in the difference from night to night and between the Delaware — Detroit and Delaware — Buffalo temperatures.

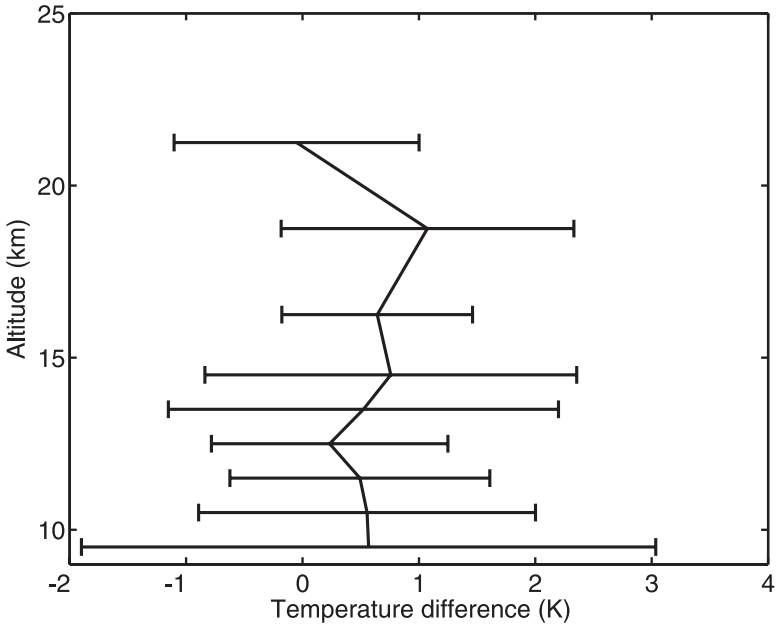

is different at these two wavelengths. The lidar system optical efficiency difference is difficult to measure accurately as it requires the experimental simulation of the backscattered light. The optical attenuation of the atmosphere at the two wavelengths from one range bin to the next cannot reasonably be measured, so an external calibration is required.

Temperature

Initial calibrations were carried out by comparing the lidar temperature measurements with the measurements made by 10 radiosondes launched from the PCL facility (Delaware Observatory, 42.87 N, 81.38 W) during July and August 2000. However, it was evident that a longer data set was necessary to provide information on seasonal effects rather than biasing the calibration to a brief period in the summer.

The temperature profiles measured by the radiosondes launched from the Delaware Observatory were compared to those measured by radiosondes launched from Detroit (DTX, 42.70 N, 83.47 W), which is approximately 160 km west–south–west of London, and Buffalo (BUF, 42.93 N, 78.73 W) which is about 200 km east of London [8]. Initially, each of the Delaware radiosondes was compared to two corresponding radiosondes, one launched from Detroit, and one from Buffalo. The launch times of the Delaware and US radiosondes did not correspond exactly; the maximum difference being 6 h. On average, the temperature comparisons between the Delaware radiosonde measurements and the US radiosonde measurements agreed quite well, see Fig. 2. The mean temperature difference over all flights and for altitudes above 9 km is 0.52 K. The Delaware radiosondes reached an average altitude of 21 km, while the US radiosondes consistently reach altitudes above 25 km, thus, the US radiosondes offer a more complete data set for the calibration of the PCL. For all but 1 of the 141 nights of PCL measurement from 1999 to 2003 used in this study, there are four radiosonde measurements available from the US sites, two each from Buffalo and Detroit at 0 and 12 UT.

As the lidar temperature profiles are calculated from the measured relative density profiles, it was decided to determine a calibration correction for measured PCL density profiles using the radiosonde

© 2007 NRC Canada

measurements rather than determining the correction for the temperature profile directly. Measurements from each observing period, typically 2 to 7 h, were averaged to form a single density profile with 250 m altitude bins. The density profiles were subsequently smoothed in altitude, using a seven point numerical filter. The four radiosonde measurements, DTX and BUF, launched at 0 and 12 UT were used in the comparison with each PCL density profile.

After some investigation it was found that the required density correction was a function of the focus of the receiving telescope. The telescope focus changes with rotation speed of the PCLs liquid-mirror telescope (LMT) and with ambient temperature. The PCL LMT uses a closed-loop control system which maintains the average speed of the mirror to within about 50 ppm of a preset speed. This is sufficient to limit focal length changes to less than ± 0.05 mm (over a focal length of 5.125 m). Larger changes in the focus of the telescope are produced by changes in the ambient temperature; the tripod that supports the detector box at the focus of the LMT is constructed of aluminium so that the detector box moves, along the optical axis, as the ambient temperature changes. A 5 K change in the temperature of the tripod will move the field-stop, which is mounted in the base of the detector box, 0.57 mm with respect to the LMT. Thus, a 5 K temperature increase is equivalent to refocusing the system from infinity to about 50 km altitude. The efficiency of the detection system, for backscatter from 10 km, for the LMT focused at infinity is 94.5% and for the LMT focused at 50 km this increases to 97.6%.

A measure of the vertical location of the detection system focus can be found by looking at the nitrogen Raman signal received in the altitude range from 3 to 5 km. For this altitude region small changes in the focus of the telescope leads to large changes in the received signal. Since the transmitted laser power can also affect the signal level a normalized signal, defined as the log of the signal from 3 km divided by the signal from 12 km, is calculated.

The density profiles measured on each night were divided into four groups based on their normalized signal. For each of these groups the nightly averaged PCL measured density was compared to the density from the radiosondes and a correction profile determined. The correction profiles for the data within each of the four groups were then averaged to obtain four correction profiles. A fifth-order polynomial was fitted to each of the correction profiles resulting in four corrections that could be applied to each nightly-averaged measurement. This provides the required corrected-density profile. The correction polynomials are constrained to be equal to unity at an altitude of approximately 28 km, since aerosols seldom affect the density measurements at these altitudes.

The polynomial corrections were applied to the densities measured on each of the 141 nights and the temperature was then determined from these corrected density profiles. The accuracy of the correction was subsequently determined through a comparison with the radiosondes launched from Buffalo and Detroit, as well as with the CIRA [9] atmospheric model. The mean difference in temperature between the lidar and radiosonde measurements was averaged over altitude intervals of 1 km. When the lidar's measurements were affected by clouds, the lidar measurements were truncated above the altitude of the cloud tops.

Sufficient measurements exist to compare the PCL-corrected average temperatures in May through August to the average temperatures measured by radiosondes and the CIRA model temperatures (Fig. 3). In Fig. 3, the error bars on the lidar temperatures are not the statistical uncertainly inherent in the lidar measurements due to photon counting, but represent the geophysical variability of the temperature for that month, they are the RMS deviation from the monthly mean temperature. With the PCL's large power-aperture product the statistical uncertainties in the measurements are a small fraction of the geophysical variability over the night. Note: during May 1999, all the radiosondes launched from Detroit and Buffalo achieve altitudes of only $\sim$16 km, creating a slight discontinuity in the mean radiosonde temperature at this altitude.

Differences between the lidar temperatures and those measured by the radiosondes are caused in part by temperature variation between the Delaware Observatory and the Buffalo and Detroit radiosondes. The error due to the seeding of the lidar temperature retrieval algorithm is small for the temperatures

© 2007 NRC Canada

Fig. 3. Monthly averaged temperature profiles measured by the PCL (continuous lines) and US National Weather Service's radiosondes (dotted lines) for measurements taken in the period 1 July 2000 to 30 November 2003. The predictions of the CIRA model are shown for comparison (broken lines). The error bars are not the measurement errors in the lidar measurements; rather they are the RMS deviation of the individual temperatures from the monthly mean temperature, minus the typical measurement uncertainty, and so represent the geophysical temperature variability.

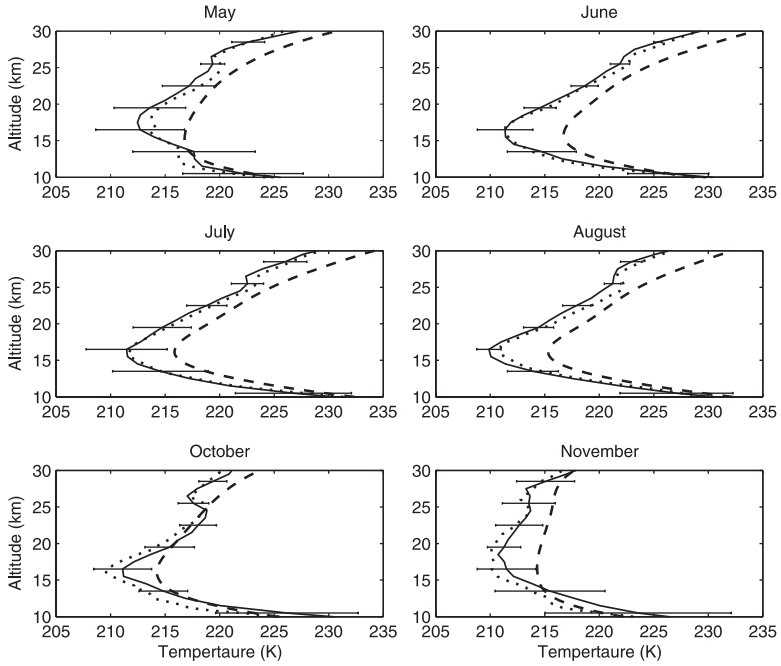

presented, even at the highest altitudes. This error can be estimated by considering the difference between the PCL Rayleigh and CIRA temperatures at 40 km and calculating the temperature error propagated down to 30 km. Using this procedure the error at 30 km caused by seeding the temperature retrieval using CIRA is estimated to be $<$1.5 K. The typical statistical uncertainly in the individual nightly averaged temperature profiles is about 2 K at 30 km, decreasing to about 0.2 K at 20 km.

Differences between the lidar and radiosonde measurements can be expected due to the spatial and temporal differences in the measurements. The lidar measurements are averaged over typically 4–5 h, sometimes up to 10 h, while the radiosondes measurements are a series of instantaneous measurements taken sequentially at increasing altitudes. The 0 UT radiosondes are flown at about the time the lidar measurements start in the winter, however, in the summer, the lidar measurements do not start until after 2 UT. Diurnal temperature variations are, therefore, likely to affect this calibration.

Seasonal variation in the atmospheric aerosol content may also play a role in the reduced accuracy of the correction in the spring, fall, and winter. PCL measurements from the summer months (June–August) account for a disproportionate 58% of the 141 nights. Thus, the correction is based predominantly on summer measurements, and might not perform as well at other times of the year. This is reflected in the correction being less accurate below 15 km for many nights from mid-October through to the end of May and in the May, October, and November lidar temperature averages, Fig. 3, being further from the radiosonde averages than for the months of June–August. This is to be investigated further in an effort to reduce the error in the correction in the nonsummer months from the current level of $\sim$2 K to the level of the summer months correction, which is $<$0.5 K.

Having established a correction for PCL Raman temperature measurements allows the temperature to be measured with the PCL Raman lidar on short-time scales; temperature fluctuations on the order

© 2007 NRC Canada

Fig. 4. Tropopause and lower stratospheric temperatures for the night of 10 July 2005. The contour interval is 2 K.

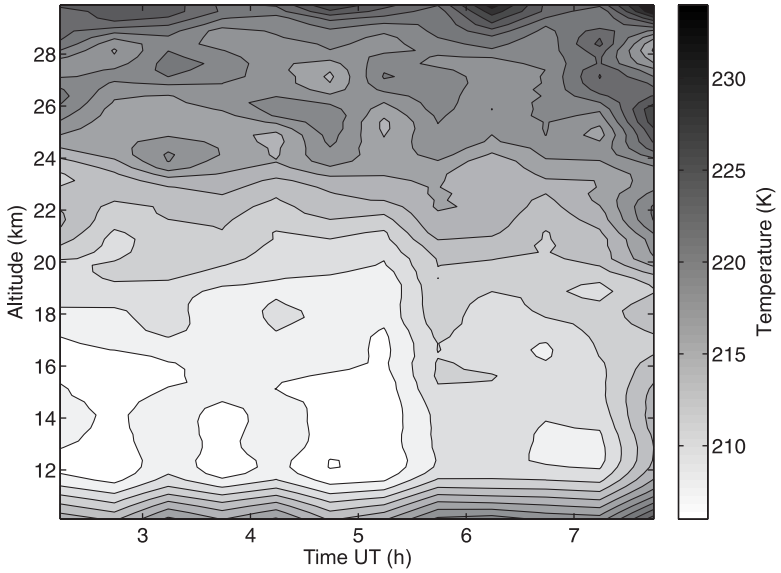

of 5 min can be measured at altitudes below about 20 km. Figure 4 shows the temperature as a function of time and height for the night of 10 July 2005. The temperature profiles used to construct this Fig. 4 are averaged over 250 m in height and 30 min in time. A seven point filter, in height, was also applied. The measurements show significant cooling over the night in the lower stratosphere, while the upper stratospheric temperature remains relatively constant.

Initial comparisons between the temperatures derived using the Rayleigh and Raman techniques show good agreement. Figure 5 shows a comparison of the PCL Rayleigh and Raman temperatures for a single night, 29 June 2003. The Raman temperature profile has had the top 10 km removed. The fluctuations in the Raman temperature profile are due to statistical variations associated with photon counting.

Water vapour

Whiteman [10] derives an expression for the water-vapour mass-mixing ratio, W_{mass} from Raman lidar measurements of the backscattered intensity from nitrogen and water-vapour molecules as

$$W_{\text{mass(g/kg)}} = \frac{k_{N_2}}{k_{H_2O}} \cdot \frac{\sigma_{N_2}}{\sigma_{H_2O}} \cdot \frac{M_{H_2O}}{M_{\text{dry}}} \cdot \frac{n_{N_2}}{n_{\text{dry}}} \cdot \Delta^{\omega}(z) \cdot \frac{N_{H_2O}(z)}{N_{N_2}(z)} \tag{1}$$

where k is the detection system optical efficiency, σ (T) is the Raman differential cross section, M is the molecular mass for water vapour or dry air (g/mol), n_{N_2}/n_{dry} is the number density ratio of nitrogen to dry air, $\Delta^{\omega}(z)$ is the ratio of the atmospheric transmission at 607.3 nm to that at 660.3 nm, and $N(z)$ is the lidar-measured backscattered intensity.

Raman water-vapour mixing-ratio measurements require an external calibration to correct for instrumental effects, detection efficiency differences for the two channels, and for atmospheric transmission differences between the two wavelengths. Previously, both radiosonde [11] and microwave radiometer [12] water-vapour measurements have been used for this calibration. In addition, a method using scattered solar light has also been used [13]. There are also many instances where water-vapour measurements made with Raman lidar have been compared to measurements made other techniques [14].

© 2007 NRC Canada

Fig. 5. Comparison between the temperatures determined by the PCL Rayleigh and Raman lidars. The measurements are averaged over the 6 h period starting at 2:15 UT on 29 July 2003. The statistical uncertainties in the Rayleigh temperatures are insignificant at the altitudes shown.

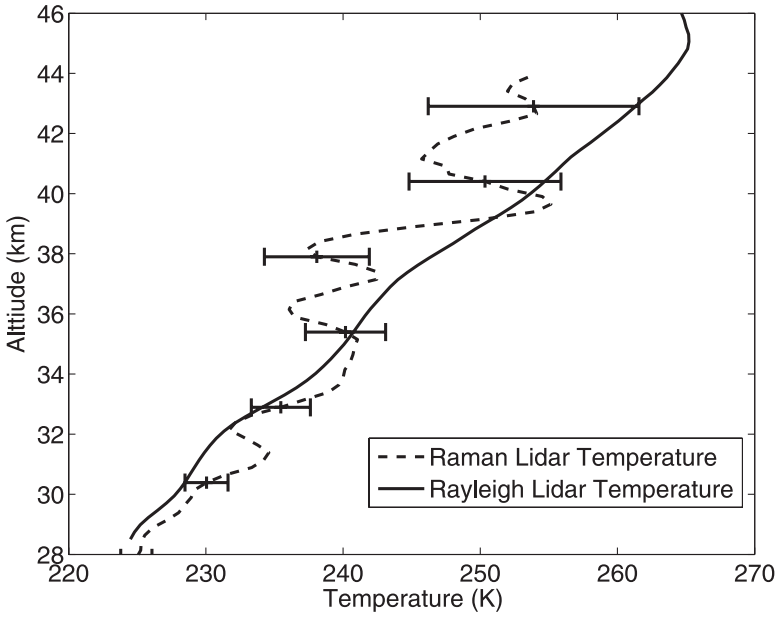

An initial calibration of the PCL water vapour system was undertaken by combining the measured optical characteristics of the instrument, using MODTRAN to estimate the required atmospheric calibration factor, and using published values for the Raman backscatter cross sections of nitrogen and water vapour [15]. The optical layout of the PCL detection system is shown in Fig. 1.

The neutral density filter in the Raman nitrogen channel allows this detection system to operate below saturation at all altitudes. Based on the measured spectral properties of the dichroic beam splitters and interference filters, and the manufacture's specified quantum efficiencies of the photomultipliers, the ratio of the detection efficiencies at the two Raman wavelengths is calculated to be 0.40. The efficiency of the water-vapour channel is higher due to the neutral density filter in the nitrogen channel. It is difficult to estimate the uncertainty in this correction factor as the uncertainty in the quantum efficiencies is unknown.

As the optical transmission of the atmosphere differs from 607 nm to 660 nm, the relative intensities of the measured backscatter from nitrogen and water vapour must be corrected. To account for this difference we use MODTRAN, a numerical model of atmospheric transmission to determine a correction. It should be noted that the transmitted 532 nm laser beam is attenuated as it propagates up through the atmosphere causing the intensity of the backscatter from both nitrogen and water vapour to decrease with altitude. However, this attenuation does not change the ratio of the intensity of the backscattered radiation at the two wavelengths. The initial PCL calibration used MODTRAN with input appropriate for a rural aerosol model, 23 km visibility, and no cloud cover to estimate the atmospheric transmission at the two wavelengths. The ratio of the transmission at the two wavelength decreases monotonically by about 6% between the surface and 40 km altitude. The cross section of the Raman-scattering process is different for each type of molecule and must be taken into account when using Raman lidar to determine the ratio of one species to another. For the initial calibration, the cross section for water vapour was taken to be 6.8 times that of nitrogen [15].

The above factors were used as an initial calibration in the water-vapour retrievals to be compared

© 2007 NRC Canada

Fig. 6. The average difference between the corrected PCL water vapour measurements (mass mixing ratio) and the US radiosonde measurements.

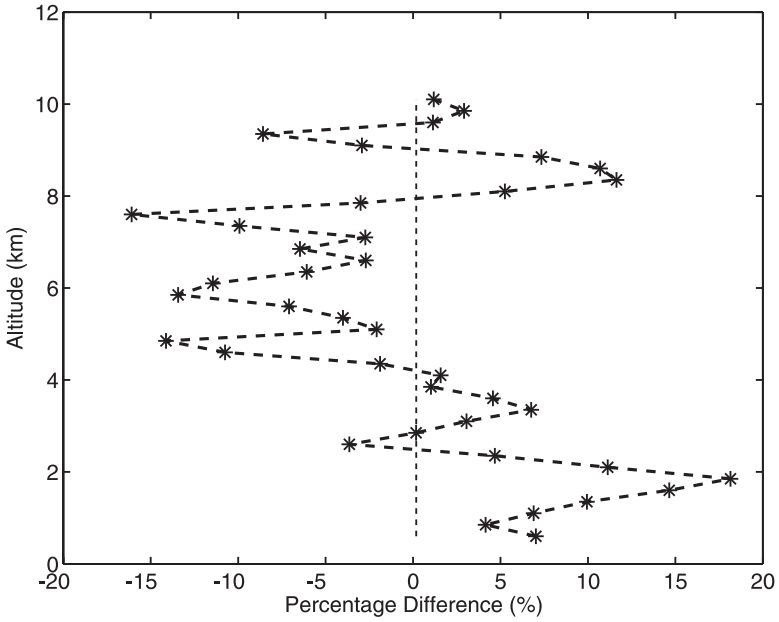

with the radiosonde measurements. PCL measurements used in a second calibration include 37 nightly averaged measurements acquired during the period 1 July 2000 to 31 December 2003. A least-squares-fitting procedure was used to scale the lidar measurements of water vapour to the average of two of those of the US sondes, the Detroit 0 UT and Buffalo 12 UT. On average, these two sonde flights showed the best agreement with the PCL measurements, reflecting the fact that air masses typically move across southwestern Ontario in roughly an eastward direction. The altitude range of the fitting was 4.6 km to 6.1 km. It was found that at lower altitudes, particularly in the lower 2 km, the correlation in water-vapour concentration between the radiosondes and the lidar was highly variable. It is well known that at low relative humidity the water-vapour sensors on the radiosondes suffer from hysteresis [16]. To avoid this problem the upper altitude used in this comparison was set at 6.1 km.

The ratios of the PCL to the US radiosonde water-vapour measurements for each of the 37 nightly averaged measurements are relatively constant having a mean of 0.996 and a standard deviation of 0.280. Hence, our initial (calculated) calibration factor, based on reasonable assumptions about our instrument, was within 0.5% of the experimentally determined value. The average difference between the lidar measurements, with this scaling factor applied, and the radiosonde measurements, is shown in Fig. 6. Figure 6 shows that the corrected lidar measurements are too large below 2 km and too small between 4 and 8 km, but in general agree to within about $\pm 12\%$. This indicates that there may still be a residual height-dependent error in the correction. However, the radiosonde measurements used as a reference for determining the lidar's calibration are not without errors. The radiosondes are known to have a dry bias of about 5%, as well as peak-to-peak variations of up to 25% between radiosondes [17].

Figure 7 show a time–height contour of tropospheric water vapour on 1 May 2002. The water-vapour mixing ratio is highly variable, which highlights two important points. First, the geophysical variability on a night is considerable, and these variations are a part of the difference between the water-vapour and radiosonde measurements. Second, the high variability showcases the advantage of the lidar's temporal–spatial resolution for continuously monitoring water vapour throughout the night over an extended altitude range.

© 2007 NRC Canada

Fig. 7. Time-height contours of PCL tropospheric water-vapour measurements from the night of 1 May 2002. The contour interval is 0.2 g/kg.

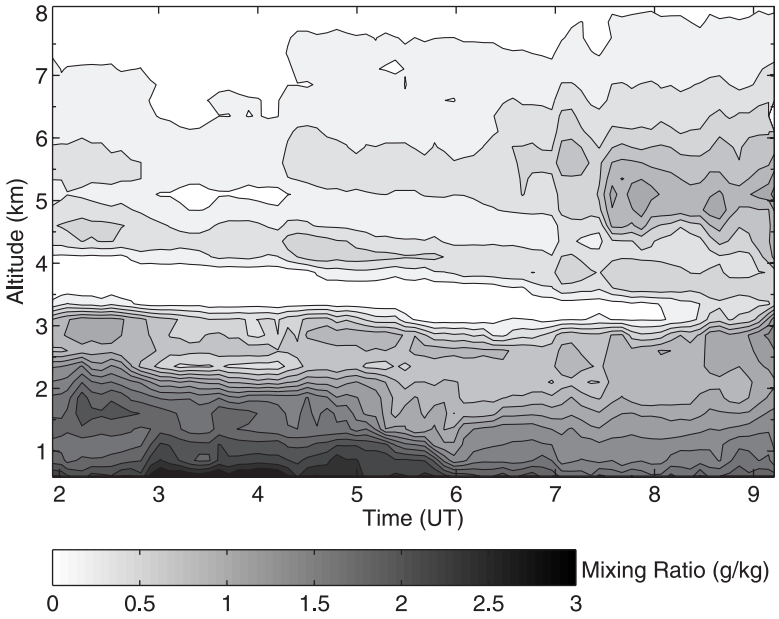

Conclusions

We have completed an initial calibration of the PCL Raman temperature and water-vapour systems. A major difficulty in undertaking this calibration was the use of radiosondes measurements from remote locations which added some difficulty to quantifying the uncertainty in the calibration.

The calibration of the PCL Raman temperatures allows the lower limit of PCL temperatures to be extended from approximately 30 km down to about 10 km, giving an overall altitude range for PCL temperature measurements extending from about 10 km to over 100 km. These measurements will allow further studies of the short-term gravity wave induced and the long-term climatic temperature changes in the upper troposphere, stratosphere, mesosphere, and lower thermosphere.

The calibration of the PCL Raman water-vapour system allows absolute water-vapour concentrations to be determined, allowing detailed studies of the evolution of water-vapour concentrations over an individual night and over seasons and years. The high-power-aperture product of the lidar allows water-vapour measurements to extend up into the lower stratosphere, allowing simultaneous measurements of temperature and water vapour in this region.

References

1. R.J. Sica, S. Sargoytchev, P.S. Argall, E.F. Borra, L.Girard, C.T. Sparrow, and S. Flatt. App. Opt. **34**, 6925 (1995).
2. D.A. Leonard. Nature, **216**, 142 (1967).
3. J.A. Cooney. Appl. Phys. Lett. **12**, 2, 40 (1968).
4. A. Hauchecorne and M.L. Chanin. Geophys. Res. Lett. **7**(8), 565 (1980).
5. T. Shibata, M. Kobuchi, and M. Maeda. App. Opt. **25**(5), 685 (1986).
6. C.S. Gardner, D.C. Senft, T.J. Beatty, R.E. Bills, and C.A. Hostetler. World Ionosphere/Thermospher Study (WITS) Handbook. Vol. 2. *Edited by* C.H. Liu. SCOSTEP Secretariat, University of Illinois, Urbana, Ill. 1989. pp. 148-187.
7. P. Keckhut, M.L. Chanin, and A. Hauchecorne. Appl. Opt. **29**(34), 5182 (1990).
8. http://raob.fsl.noaa.gov/

© 2007 NRC Canada

9. E.L. Fleming, S. Chandra, M.R. Schoerberl, and J.J. Bennett. NASA Tech. Memorand. 100697. 1988.
10. D.N. Whiteman, S.H. Melfi, and R.A. Farrare. Appl. Opt. **31**, 3068 (1992).
11. R.A. Ferrare, S.H. Melfi, D.N. Whiteman, K.D. Evans, F.J. Schmidlin, and D.O. Starr. J. Atmos. Ocean Tech. **12**(6), 1177 (1995).
12. M.N. England, R.A. Ferrare, S.H. Melfi, D.N. Whiteman, and T.A. Clark. J. Geophys. Res: Atmos. **97**(D1), 899 (1992).
13. V. Sherlock, A. Hauchecorne, and J. Lenoble. Appl. Opt. **38**(27), 5816 (1999).
14. R.A. Ferrare, E.V. Browell, S. Ismail, S.A. Kooi, L.H. Brasseur, V.G. Bracket, M.B. Clayton, J.D.W. barrick, G.S. Diskin, J.E.M. Goldsmith, B.M. Lesht, J.R. Podolske, G.W. Sachse, F.J. Schmidlin, D.D. Turner, D.N. Whiteman, D. Tobin, L.M. Miloshevich, H.E. Revercomb, B.B. Demoz, and P. Di Girolamo. J. Atmos. Ocean Tech. **21**(12), 1790 (2004).
15. H.W. Schrotter and H.W. Klockner. *In* Raman spectroscopy of gases and liquids. *Edited by* A. Weber. Springer-Verlag, Berlin. 1979. Chap. 4. pp. 123–166.
16. C.G. Wade. J. Atmos. Ocean Tech. **11**(3), 687 (1994).
17. D.D. Turner, B.M. Lesht, S.A. Clough, J.C. Liljegren, H.E. Revercomb, and D.C. Tobin. J. Atmos and Ocean Tech. **20**(1), 117 (2003).

© 2007 NRC Canada